Resonant Tunneling into a Biased Fractional Quantum Hall Edge

M. Grayson,[1,2,*] D. C. Tsui,[1] L. N. Pfeiffer,[3] K. W. West,[3] and A. M. Chang[3,4]

[1]*Department of Electrical Engineering, Princeton University, Princeton, New Jersey 08544*
[2]*Walter Schottky Institut, Technische Universität München, D-85748 Garching, Germany*
[3]*Bell Laboratories, Lucent Technologies, 600-700 Mountain Avenue, Murray Hill, New Jersey 07974-0636*
[4]*Department of Physics, Purdue University, West Lafayette, Indiana 47907-1396*

(Received 11 October 2000)

We observe resonant tunneling into a voltage biased fractional quantum Hall effect (FQHE) edge, using atomically sharp tunnel barriers unique to cleaved-edge overgrown devices. The resonances demonstrate different tunnel couplings to the metallic lead and the FQHE edge. Weak coupling to the FQHE edge produces clear non-Fermi liquid behavior with a sixfold increase in resonance area under bias arising from the power law density of states at the FQHE edge. A simple device model uses the resonant tunneling formalism for chiral Luttinger liquids to successfully describe the data.

DOI: 10.1103/PhysRevLett.86.2645 PACS numbers: 73.43.Jn, 71.10.Pm, 72.20.My

Studies of resonant tunneling at the fractional quantum Hall effect (FQHE) edge have long sought to demonstrate clear non-Fermi-liquid behavior. The correlated FQHE state [1] is predicted to host an interacting one-dimensional electronic system at its edge called a chiral Luttinger liquid [2], yet conclusive evidence for Luttinger liquid behavior in resonant tunneling measurements has proved elusive [3–5]. A simple measurement of the resonance line shape can theoretically resolve the character of the leads [6–9], but in practice the subtle difference between a Fermi-liquid (FL) and Luttinger-liquid (LL) line shape is beyond experimental resolution [4]. One must therefore introduce an external energy scale, e.g., temperature, to probe the character of the resonance. Temperature dependent studies of gate tuned resonances in a disordered FQHE point contact [4] showed linewidths consistent with the expected $T^{2/3}$ scaling, but only over a factor of 3 in temperature—not convincingly different from the linear fit that a conventional FL resonance would produce. In this Letter we demonstrate another energy scale besides temperature that can reveal non-FL behavior, namely an external voltage bias.

New questions about the very nature of the FQHE edge have been posed by recent (nonresonant) tunneling experiments by the authors [10–12]. When tunneling into a sharp FQHE edge the power law current-versus-voltage characteristic anticipated for the chiral LL was seen for a *whole continuum of filling factors.* Depending on sample quality, the power law exponent, α, would vary linearly with the reciprocal of the filling factor, $1/\nu$ [11], or exhibit a plateau structure near $\alpha \sim 3$ [12]. While these results provided strong evidence for a chiral LL at $\nu = 1/3$, away from $\nu = 1/3$ they deviated from the theoretically expected behavior [13] stimulating a host of recent theoretical work [14]. The discovery and characterization of the resonance in this Letter promise a new criterion for understanding the physics of the sharp FQHE edge.

This new tunneling resonance occurs in the same type of cleaved-edge overgrown [15] tunnel junction previously studied by the authors [10–12,16] between a bulk doped metal and a FQHE edge (device inset, Fig. 1). The resonance itself most likely arises from an unintentionally introduced impurity state in the barrier. Because of the sharp and energetically tall (100 meV) barrier, we can for the first time characterize the response of the resonance under dc bias, whereas with gate defined tunnel structures a moderate dc bias distorts the soft tunneling barrier. The quantum wells of samples R and M had two-dimensional (2D) carrier densities of $n_e = 1.08$ and 0.89×10^{11} cm^{-2}, and mobilities of $\mu = 2.9$ and 1.8×10^6 cm^2/V s, respectively. These were simultaneously cleaved and edge grown with a 90 Å $Al_xGa_{1-x}As$ barrier ($x = 0.1$) , followed by 150 Å undoped GaAs and 0.5 μm bulk doped GaAs, $n^+ \sim 2 \times 10^{17}$ cm^{-3}.

To measure conductance, G, we applied an 8 μV ac rms square wave and measured the resulting current with a lock-in amplifier while sweeping the magnetic field, B (Fig. 1). The ac voltage was chosen to match our thermally limited resolution at base temperature, 25 mK ($V_{ac} \sim 2\pi k_B T$) [6]. Since the exact density profile at the edge

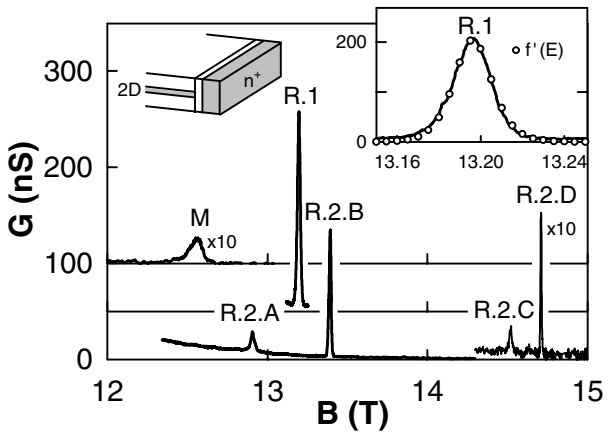

FIG. 1. Samples M, R.1, and R.2. Inset right: R.1 with derivative Fermi function. Inset left: Device.

is uncertain [17] we explicitly refer to all filling factors as ν_{bulk}. For sample R, we label the first and second cooldowns as R.1 and R.2, and append an additional suffix for multiple resonances (R.2.A, R.2.B, etc.).

Sample M in Fig. 1 showed a resonance at $\nu_{\text{bulk}} = 0.294$, and R.1 showed the strongest resonance at $\nu_{\text{bulk}} = 0.338$. For the second cooldown R.2, we see four resonances at $\nu_{\text{bulk}} = 0.346$, 0.333, 0.307, and 0.303 from left to right, respectively. Other samples measured showed no detectable resonances. For the resonance R.1 we also measured temperature dependence (Fig. 2). With increasing T the resonance linewidth broadens and the peak height decreases relative to a rising background conductance (Fig. 2, inset).

To measure bias dependence, a fixed dc bias from -40 to $+40$ μV was added to the ac signal and differential conductance, dI/dV, was measured as a function of B (Fig. 3). With bias the background conductance increases due to the power law density of states, shifting the curves upwards. For our sign convention we electrically ground the 2D and apply the signed voltage to the n^+ electrode. Starting with R.1 (Fig. 3, right), the peak splits under bias into a tall and a short peak with the tall peak shifting farthest from center and the total separation in B proportional to the applied voltage. The total area subtended by the two peaks relative to the background increases only slightly under bias. Measuring the bias dependence of another resonance R.2.A (Fig. 3, left), instead of splitting this peak broadens into a lopsided single peak that leans to the right for positive bias and to the left for negative bias. Most notably, the area subtended by the resonance relative to the background conductance increases by a factor of 6 under 30 μV bias, an altogether different qualitative behavior from R.1.

To begin our analysis, we relate the magnetic field to an energy scale using two different methods. First note (Fig. 1, inset) that the line shape for R.1 can be scaled to fit the derivative of a Fermi function, $-f'(E) = \frac{1}{4k_BT}\,\text{sech}^2(\frac{E}{2k_BT})$, the line shape expected for a resonance fed by a Fermi liquid lead. Dividing the calculated thermal linewidth, $\Delta E = 4k_BT\,\text{arccosh}(\sqrt{2})$ by the linewidth of the observed resonance ΔB, we deduce from thermal measurements a scaling coefficient β_T:

$$|\beta_T| = \left|\frac{dE}{dB}\right| = \frac{\Delta E}{\Delta B} = 0.42\ \text{meV/T}. \quad (1)$$

Alternatively, since the B-field separation between peaks in Fig. 3 is linear with applied bias, we can empirically assign from voltage bias measurements a coefficient, β_V:

$$|\beta_V| = \left|\frac{dE}{dB}\right| = \frac{eV_{\text{bias}}}{B_{\text{peak2}} - B_{\text{peak1}}} = 0.43\ \text{meV/T}. \quad (2)$$

The clear agreement of these coefficients suggests that the energy of the resonant state, E_r, is being swept through the chemical potential in proportion to the magnetic field by a single coefficient $\beta = \frac{dE_r}{dB}$, with the resonant state producing a conductance peak whenever it passes the chemical potential in either lead.

Turning to the temperature dependent measurements of R.1 (Fig. 2, inset), the resonance broadens roughly linearly in T, and the peak height drops relative to the background as $1/T$ consistent with thermal broadening of a FL resonance. The background conductance, however, behaves as a *power law* in temperature with the same LL-like exponent reported previously [10–12], implying we have a FL-like resonance *on top of a LL-like background.*

The key to understanding this behavior lies in the *relative* coupling strength of the resonance to the two leads. We define Γ_{FL} as the tunnel coupling strength from the resonant state to the n^+ lead, and Γ_{QH} as the coupling to the quantum Hall lead. Overall the resonance is weakly

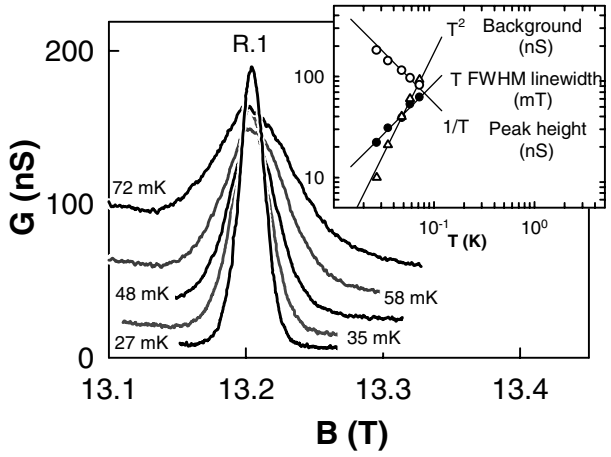

FIG. 2. Temperature dependent conductance of R.1. Inset: behavior of peak structure.

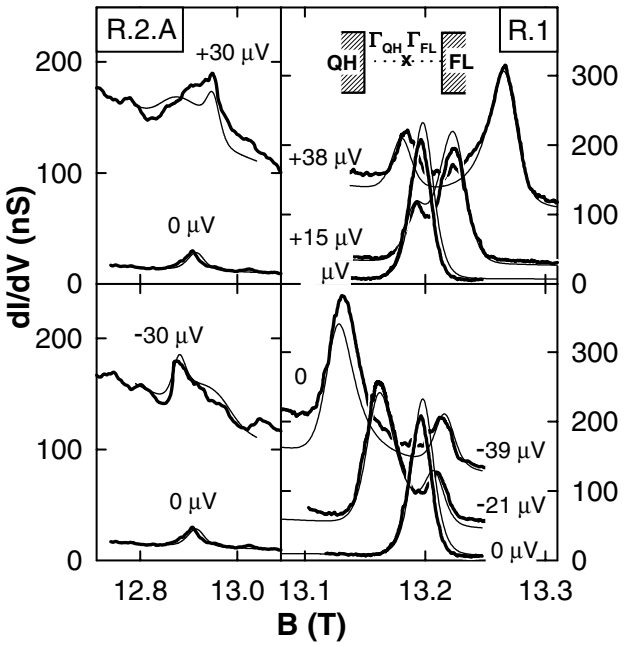

FIG. 3. dI/dV vs B at fixed dc bias for R.2.A and R.1. Data in bold, fits in fine lines. Inset, top: the coupling Γ_{QH} and Γ_{FL} of the resonant state to the quantum Hall and Fermi liquid leads.

coupled since the strongest peak is a factor of 100 smaller than the perfect resonant conductance, $e^2/2h$; but as pointed out by Kane [18], when the *relative* coupling to the two leads is different, the tunnel conductance will be determined principally by the *most weakly coupled lead.* To develop our intuition, we will discuss the limit case where the stronger coupled lead combines with the resonance to act as a delta function at the resonance energy E_r. Under bias V to the strongly coupled lead, a current I_r then results from the weak coupling Γ to the density of states in the remaining lead $\frac{dn}{dE}$ [with Fermi distribution $f(E) = \frac{1}{e^{E/kT}+1}$]:

$$I_r(E_r) = \Gamma \frac{e}{h} \frac{dn}{dE}(E_r) \times \{[1 - f(E_r)]f(E_r - eV) - f(E_r)[1 - f(E_r - eV)]\}. \quad (3)$$

The real space position of the resonance in the tunnel junction causes the resonance energy, E_r, to depend on bias. Assuming the resonance is bound to the local band structure with energy βB_0, we define the lever arm parameter λ as the fraction of the applied bias that falls to the weakly coupled side of the resonance. Combining this with the previously noted B dependence gives the following function for the resonance energy:

$$E_r(V, B) = \lambda eV + \beta(B - B_0). \quad (4)$$

Substituting this into Eq. (3) and differentiating with respect to voltage gives us the differential conductance

$$\frac{dI_r}{dV}(E_r) = \Gamma \frac{e^2}{h}\left[\lambda \frac{d^2n}{dE^2}(E_r)\{\cdots\} - \lambda \frac{dn}{dE}(E_r)f'(E_r) - (1 - \lambda)\frac{dn}{dE}(E_r)f'(E_r - eV)\right], \quad (5)$$

where the expression in braces $\{\cdots\}$ is that from Eq. (3). Since E_r is linear with B from Eq. (4), we can compare $\frac{dI_r}{dV}(E_r)$ from Eq. (5) with the data, $\frac{dI_r}{dV}(B)$ from Fig. 3.

In what we call the Fermi-liquid coupled (FLC) limit, $\Gamma_{\mathrm{FL}} \ll \Gamma_{\mathrm{QH}}$, the resonance is more weakly coupled to the n^+ lead so the FL density of states enters into Eq. (5). We neglect the first term in Eq. (5) relative to the others since for a FL at low T, $\frac{d^2n}{dE^2} \ll \frac{dn}{dE}f'(E)$. Approximating $\frac{dn}{dE} = n_0$, the conductance peaks occur when the argument of f' is zero. The second term produces a peak weighted by λ when the resonance is aligned with the n^+ chemical potential, $B = -\frac{\lambda e}{\beta}V + B_0$, and the third term produces a peak weighted by $(1 - \lambda)$ when the resonance is aligned with the chemical potential of the FQHE edge, $B = +\frac{(1-\lambda)e}{\beta}V + B_0$. Looking at Fig. 3, the lever arm model clearly accounts for the zero bias line shape of $-f'(E_r)$ and for the existence under bias of two peaks of differing height shifted in B proportional to their heights.

In the contrasting quantum Hall coupled (QHC) limit $\Gamma_{\mathrm{QH}} \ll \Gamma_{\mathrm{FL}}$, the resonance is more weakly coupled to the FQHE edge and the power law density of states enters into Eq. (5). Here the resonance peak from the second term in Eq. (5) is completely suppressed because the density of states $\frac{dn}{dE}(E_r)|_{E_r=0} = E_r^{\alpha-1} = 0$, vanishes when the resonance is aligned with the FQHE chemical potential. We therefore expect only a *single peak* from the third term when E_r is aligned with the n^+ chemical potential. The first term now contributes a nonnegligible conductance proportional to the derivative of the density of states $\frac{d^2n}{dE^2}$ between the two resonance centers. For $\alpha = 3$ at a $1/3$ FQHE edge, this additional conductance goes as $\frac{dI}{dV} \sim E_r^{\alpha-2} \sim E_r$, rising linearly with B as it approaches the single resonance peak (Fig. 3, left).

Beyond differences in line shape, the most striking qualitative difference between the QHC and FLC limits is the (non)conservation of resonance area under bias. In the FLC limit, the total integral of the resonance area is constant, $\int \frac{dI}{dV}(E_r)\,dE_r = \Gamma \frac{e^2}{h} n_0$, independent of bias. In the contrary QHC limit the power law density of states $\frac{dn}{dE} \sim E^{\alpha-1}$ leads to a simple power law dependence of the resonance area on voltage bias (at zero temperature): $\int \frac{dI}{dV}(E_r)\,dE_r \sim V^{\alpha-1}$. At finite temperature, Fig. 3, left, shows that this strong bias dependence remains, with a factor of $\sim$6 increase in resonance area at 30 μV. Together, the asymmetric line shape and nonconservation of resonance area under bias convincingly demonstrate the presence of a non-Fermi liquid resonance.

To simulate finite Γ_{FL} and Γ_{QH}, we adapt the resonance formalism of de C. Chamon and Wen [7] for sequential tunneling between biased chiral LL's, keeping the Luttinger parameter of one channel $g = 1/3$ and changing the parameter of the other channel to $g = 1$ to represent a FL. We then reapply our lever arm model, using a new device lever arm parameter λ' as that fraction of voltage bias on the n^+ side of the resonance. Up to a scaling factor for the Γ's, our model has a unique solution for a given sign of β since the three independent quantities β, λ', and $\Gamma_{\mathrm{QH}}/\Gamma_{\mathrm{FL}}$ are parametrically determined by fitting three structural features: the left and right peak positions, and the ratio of peak heights. The background conductance has no fit parameters since it obeys the well-known power law with voltage, and exponential decay with B [10,11].

The simulated resonance curves are plotted against the data in Fig. 3 with the four fit parameters listed in Table I. The factor of area increase under bias V_{bias} is also listed for both experiment (Σ_{exp}) and fit (Σ_{fit}). Using the coupling constants and area conservation as an indicator of the coupling limit, we see that resonances R.1 and R.2.B are near the FLC limit with $\Gamma_{\mathrm{FL}} < \Gamma_{\mathrm{QH}}$, and a modest 50% and 70% increase in area with bias, respectively. The temperature dependence of R.1 is also consistent with calculations, with the experimental 30% increase in area from $T = 27$ mK to 73 mK consistent with the modeled 45% increase. By contrast, R.2.A approaches the QHC limit with $\Gamma_{\mathrm{QH}} \sim \Gamma_{\mathrm{FL}}$ and the previously noted factor of 6 increase in area with bias. The sign of β is uniquely

TABLE I. Summary of resonance parameters.

	R.1 (FLC)	R.2.A (QHC)	R.2.B (FLC)
	Lever arm parameters		
λ'	0.20	0.30	0.20
β	$+0.43\frac{\text{meV}}{\text{T}}$	$-0.26\frac{\text{meV}}{\text{T}}$	$+0.59\frac{\text{meV}}{\text{T}}$
Γ_{FL}	1.3	1.0	1.0
Γ_{QH}	19.7	3.5	14.0
	Area increase under bias		
Σ_{exp}	1.5 ± 0.1	6 ± 1	1.7 ± 0.1
Σ_{fit}	1.54	5.9	1.58
V_{bias}	39 μeV	30 μeV	30 μeV

determined for R.2.A because of the lopsided single peak structure, and for R.1 and R.2.B, only the positive β solution can account for the observed increase in area.

We can explain the values of β as well as the observed sign change by carefully considering how the 2D ground energy affects the lever arm model. In the *compressible* state increasing B increases the 2D ground energy, $E_0(B) = \frac{1}{2}\hbar\frac{eB}{m^*}$, thereby lowering the 2D conduction band and leveraging the resonance energy down by the lever arm factor, λ': $\beta_{\text{comp}} = \frac{dE_r}{dB} = -\lambda'\frac{1}{2}\frac{\hbar e}{m^*}$. The resulting $\beta_{\text{comp}} = -0.26$ meV/T exactly matches the fit parameter for R.2.A suggesting that this resonance couples to a compressible edge. On the other hand in the *incompressible* state, the ground energy drops by the mobility gap Δ over the width of the plateau $\bar{B}$, changing the sign of β and setting a lower bound $\beta_{\text{incomp}} \geq +\Delta/\bar{B}$. Using measured values of $\Delta = 450$ μeV and $\bar{B} = 2$ T, we get $\beta_{\text{incomp}} \geq 0.22$ meV/T, consistent with the values for R.1 and R.2.B, and suggesting that these resonances couple to incompressible edges. With the negative β (R.2.A) and positive β (R.2.B) resonances having the same Γ_{FL}, it is even possible these neighboring resonances arise from the same resonant state which is first lowered and then raised through the chemical potential by leveraged 2D ground energy oscillations. The differences in λ' and Γ_{QH} between resonances are then explainable from differences in the screening length and tunneling character of compressible and incompressible edges. If the resonance pair R.2.A/R.2.B results from the $\nu_{\text{edge}} = 1/3$ transition and R.2.C/R.2.D from $\nu_{\text{edge}} = 2/5$, this is consistent with an edge density enhancement $\nu_{\text{edge}} \sim 1.2\nu_{\text{bulk}}$ [17].

In conclusion, we have observed and characterized the voltage dependence of a new type of resonance at a sharp FQHE edge, demonstrating clear non-FL behavior through line shape analysis and nonconservation of resonance area.

The authors are grateful to C. Chamon, M. P. A. Fisher, B. Halperin, L. Levitov, and C. Kane for insightful discussions. M. G. thanks the A. v. Humboldt Foundation for support during writing. This work was supported by the DOE and AFOSR.

*Present address: Walter Schottky Institut, Technische Universität München, D-85748 Garching, Germany.
Electronic address: mgrayson@alumni.princeton.edu

[1] D. C. Tsui, H. L. Stormer, and A. C. Gossard, Phys. Rev. Lett. **48**, 1559 (1982).
[2] X. G. Wen, Phys. Rev. B **43**, 11 025 (1991); **41**, 12 838 (1990); **44**, 5708 (1991); Phys. Rev. Lett. **64**, 2206 (1990).
[3] J. A. Simmons, H. P. Wei, L. W. Engel, D. C. Tsui, and M. Shayegan, Phys. Rev. Lett. **63**, 1731 (1989).
[4] F. P. Milliken, C. P. Umbach, and R. A. Webb, Solid State Commun. **97**, 309 (1996).
[5] V. J. Goldman and B. Su, Science **267**, 1010 (1995); I. J. Maasilta and V. J. Goldman, Phys. Rev. B **55**, 4081 (1997).
[6] C. L. Kane and M. P. A. Fisher, Phys. Rev. B **46**, 15 233 (1992).
[7] C. de C. Chamon and X. G. Wen, Phys. Rev. Lett. **70**, 2605 (1993).
[8] A. Furusaki and N. Nagaosa, Phys. Rev. B **47**, 3827 (1993); A. Furusaki, Phys. Rev. B **57**, 7141 (1998).
[9] K. Moon, H. Yi, C. L. Kane, S. M. Girvin, and M. P. A. Fisher, Phys. Rev. Lett. **71**, 4381 (1993).
[10] A. M. Chang, L. N. Pfeiffer, and K. W. West, Phys. Rev. Lett. **77**, 2538 (1996); Physica (Amsterdam) **383B**, 249 (1998).
[11] M. Grayson, D. C. Tsui, L. N. Pfeiffer, K. W. West, and A. M. Chang, Phys. Rev. Lett. **80**, 1062 (1998).
[12] A. M. Chang, M. K. Wu, C. C. Chi, L. N. Pfeiffer, and K. W. West, Phys. Rev. Lett. **86**, 143 (2001).
[13] A. V. Shytov, L. S. Levitov, and B. I. Halperin, Phys. Rev. Lett. **80**, 141 (1998); C. L. Kane, M. P. A. Fisher, and J. Polchinski, Phys. Rev. Lett. **72**, 4129 (1994); J. H. Han and D. J. Thouless, Phys. Rev. B **55**, 1926 (1997); J. H. Han, Phys. Rev. B **56**, 15 806 (1997); S. Conti and G. Vignale, Phys. Rev. B **54**, R14 309 (1996); Physica (Amsterdam) **1E**, 101 (1997).
[14] U. Zülicke, A. H. MacDonald, and M. D. Johnson, Phys. Rev. B **58**, 13 778 (1998); U. Zülicke and A. H. MacDonald, Phys. Rev. B **60**, 1837 (1999); U. Zülicke, Phys. Rev. Lett. **83**, 5330 (1999); A. Lopez and E. Fradkin, Phys. Rev. B **59**, 15 323 (1999); S.-R. E. Yang and J. H. Han, Phys. Rev. B **57**, R12 681 (1998); M. V. Milovanovic and E. Shimshoni, Phys. Rev. B **59**, 10 757 (1999); L. P. Pryadko, E. Shimshoni, and A. Auerbach, Phys. Rev. B **61**, 10 929 (2000); A. M. M. Pruisken, B. Skoric, and M. A. Baranov, Phys. Rev. B **60**, 16 838 (1999); J. E. Moore, P. Sharma, and C. Chamon, Phys. Rev. B **62**, 7298 (2000); S. Conti and G. Vignale, J. Phys. Condens. Matter **10**, L779 (1998); I. D'Amico and G. Vignale, Phys. Rev. B **60**, 2084 (1999); D. H. Lee and X.-G. Wen, cond-mat/9809160.
[15] L. N. Pfeiffer, K. W. West, H. L. Stormer, J. P. Eisenstein, K. W. Baldwin, D. Gershoni, and J. Spector, Appl. Phys. Lett. **56**, 1697 (1990).
[16] M. Grayson, C. Kurdak, D. C. Tsui, S. Parihar, S. Lyon, and M. Shayegan, Solid State Electron. **40**, 233 (1996).
[17] L. S. Levitov, A. V. Shytov, and B. I. Halperin, cond-mat/0005016.
[18] C. Kane, cond-mat/9809020.